Interaction of a Porphyrin-Containing Macrotetracyclic Receptor Molecule with Single-Stranded and Double-Stranded Polynucleotides. A Photophysical Study

Anny Slama-Schwok[‡] and Jean-Marie Lehn*

Chimie des Interactions Moléculaires, Collège de France, 11 Place Marcelin Berthelot, Paris 75005, France

Received January 10, 1990; Revised Manuscript Received May 1, 1990

ABSTRACT: Photophysical methods have been used to study the interaction with nucleic acids of a macrotetracyclic cryptand molecule, Pbiph, containing a porphyrin groups, two macrocycles, and a biphenyl bridge. Pbiph binds with a higher affinity to single-stranded polynucleotides than to double-stranded ones. This selectivity, observed by binding and competition studies, using absorption and fluorescence spectroscopy, is pH dependent. Pbiph does not intercalate into double helices and is suggested to bind into the major groove. These features, selective single-strand binding and nonintercalation, are attributed to steric effects of the bulky Pbiph molecule, resulting from the macropolyclic cryptand cage structure.

Cationic porphyrins bind to DNA in solution; their structure and the nature of the coordinated metal control the binding mechanism and their DNA base preference (Fiel et al., 1979; Pasternack et al., 1983; Carvlin & Fiel, 1983; Kelly & Murphy, 1985; Ward et al., 1986; Bromley et al., 1986; Ford et al., 1987; Geacintov et al., 1987; Gibbs et al., 1988; Strickland et al., 1988). The basis for these studies is in part related to the observation that porphyrins, like hematoporphyrin derivatives, can serve as photosensitizers for destruction of tumor cells (Brault et al., 1986; Malik et al., 1988). Covalent linkage of acridine to hemin gives compounds that exhibit antitumour effects in vivo and cleave DNA in vitro (Lown & Joshua, 1982). Attachment of a porphyrin to an oligonucleotide yields a sequence-specific cleaving molecule (LeDoan et al., 1986). Tetracationic porphyrins H_2TMPyP(4) and ZnTMPyP(4) photosensitize in vitro DNA cleavage (Kelly & Murphy, 1985). These porphyrins can cross the nuclear membrane; however, they present cytopathic activity (Gibbs et al., 1988).

This work presents the binding of a macrotetracyclic system Pbiph containing a porphyrin subunit (Hamilton et al., 1984, 1986) to single- and double-stranded polynucleotides. The porphyrin is linked by two [18]N_2O_4 macrocycles to a biphenyl group. In water, around neutral pH, the amine functions are protonated, ensuring electrostatic interaction with DNA. The bulky structure of this compound may allow a higher affinity for single-stranded polymers, owing to their larger flexibility, compared to double-helical polynucleotides. In addition, since the porphyrin is a photoactive moiety, it may induce DNA photocleavage in visible light.

Experimental Section

1. Chemicals. The chemicals, NaCl, sodium cacodylate (dimethylarsenic acid), HCl, and KI, were commercial analytical reagents (Merck). The synthetic polynucleotides, as well as the nucleosides and nucleoside mono- and triphosphates were PL Biochemicals products. Bidistilled water was used for all the solutions. The cells were either semimicro or micro quartz cells from Hellma (optical path of 1 cm for two faces and 0.4 or 0.2 cm, respectively, for the perpendicular optical faces). In the case of titrations with low Pbiph concentration, acryl cells (Sarstedt) were used, in order to reduce the adsorption on the cell walls. All stock solutions were kept in the dark, at −20 °C. The porphyrin containing macrotetracycle Pbiph has been synthetized in earlier work (Hamilton et al., 1984, 1986).

Table I: Photophysical Properties of Pbiph[a]

	dication	monocation	neutral
λ_{max} Soret band (nm)	404	394	400
ϵ (Soret) (M^{-1} cm^{-1})	2.9×10^5		1.1×10^5
λ Q bands (nm)	549, 594	530, 554, 602	502, 539, 558, 613
λ_{max} fluorescence (nm)	608, 666		617, 680
lifetime (ns)		8.3 ± 0.1	16.0 ± 0.2

[a] [Pbiph] = 0.2–10 μM, 10 mM NaCl.

2. Apparatus. The absorption spectra were recorded on Kontron spectrophotometers, Model 860 or 820. A Spex Fluorolog spectrofluorimeter with a double monochromator was used for the static emission experiments and anisotropy measurements. The spectra were corrected for the wavelength dependence of the transmission and detection systems and for the lamp fluctuation. The area under the fluorescence curves was then calculated to obtain relative fluorescence yields. The lifetimes were measured on an Edinburg Instruments 199 single photon counting fluorometer, using a hyperbaric hydrogen-filled flash lamp, which gave an instrumental response profile width at half-maximum height of 1.1 ns. Computer programs were used and fitted mono-, bi- and triexponential decay kinetics to the lifetime data. The quality of the fit was judged by reduced χ^2 and Durbin-Watson tests. Each apparatus was thermostated at (20 ± 1) °C, unless otherwise stated. In the case of low-temperature experiments, a nitrogen flow eliminated the condensation, ensuring correct absorbance and fluorescence measurements. The thermal denaturation experiments were performed by using a temperature programmer connected to the thermostat, allowing a very slow temperature increase, 0.15 deg/min.

Chemical and Photophysical Properties of Pbiph

Unmetallated porphyrins are cationic or neutral depending on the protonation of the heterocyclic nitrogen (Dolphin, 1979). The porphyrin–biphenyl macrotetracycle, Pbiph, possesses additional protonation sites, the amines of the lateral N_2O_4 rings. The corresponding pK_a values have been calculated from the pH dependence of the absorption and fluorescence

[‡] Present address: Department of Physical Chemistry, The Hebrew University of Jerusalem, 91904 Jerusalem, Israel.

0006-2960/90/0429-7895$02.50/0

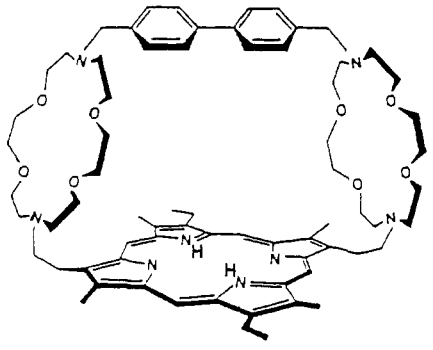

Pbiph

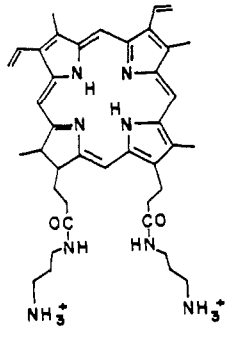

Model compound

properties summarized in Table I.

$$\text{dication} \underset{}{\overset{K_1}{\rightleftharpoons}} \text{monocation} \overset{K_2}{\rightleftharpoons} \text{neutral} \qquad (1)$$

The first pK_a of Pbiph has been obtained from absorption spectra, by the absorbance decrease at 404 nm (maximum of the dication) and the absorbance increase at 530 nm (first Q band of the monocation), and from excitation spectra, by monitoring the fluorescence at 666 nm, one of the vibronic bands of the dicationic form. An isosbestic point is observed at 387 nm, in the range $[H^+]$ = 30 mM to 3 M. The measurements have been performed at 3 M ClO_4^-, perchlorate being known as a weakly coordinating counterion. Under these conditions, $pK_1 = 0.3 \pm 0.1$. The equilibrium between monocationic and neutral forms has been studied at $[Cl^-]$ = 50 mM, by the absorbance changes at 404 and 394 nm. $pK_2 = 2.4 \pm 0.2$ has been calculated by assuming the same extinction coefficients of the dicationic form at 3 M perchlorate and at 50 mM chloride. Since an isosbestic point between monocationic and neutral forms is observed at 370 nm, the increase of fluorescence (λ_{exc} = 370 nm) at 617 and 680 nm, characteristic of the neutral form, has also been used to determine pK_2. The pK_a values obtained for Pbiph are about two pH units lower than those of other unmetalated porphyrins, for which pK_1 = 2.5–2.7 and pK_2 = 4.4–4.7 (Brault et al., 1986). These figures have been obtained at lower ionic strength, which should shift the pK_a's to somewhat higher values. The large difference of two pK units observed with Pbiph and not with a monoporphyrin model compound[1] may be indicative of large steric constraints, resulting from the "cage" structure. The pK_a values of the amines of the lateral rings could not be determined precisely, due to the precipitation of the compound at pH >8. They may be estimated to lie at pH ≥7.0. The nucleic acid binding experiments were performed at pH 4.6 and 6.6. In this range, the porphyrin subunit is neutral. The total charge of the molecule at pH 4.6 is 4+, whereas it is approximatively 2+ at pH 6.6. No evidence for dimerization has been found in the range 0.02–10 μM at 10 and 100 mM NaCl, pH 4.6–6.6, by either fluorescence or absorption measurements. Other covalently linked dimeric porphyrins also present a minimal tendency to aggregate even at a concentration as high as 100 μM (Chow et al., 1988). The fluorescence quantum yield of Pbiph at pH 6.6 has been measured by comparison with ZnTMPyP, H_2TMPyP, and quinine sulfate (Kalyanasunderam & Neumann-Spallart, 1982; IUPAC, 1986), $\phi = 5.7 \times 10^{-2}$. The quenching of the Pbiph fluorescence by iodide at constant ionic strength, 0.5 M, has been studied by steady-state measurements. The Stern–Volmer plots are linear in the iodide concentration range 2–100 mM and allow the calculation of $K_{SV} = 55 \pm 1$ M^{-1}. Taking the fluorescence lifetime of free Pbiph as 16.1 ns, the quenching rate constant by iodide is $k_q = 3.4 \times 10^9$ M^{-1} s^{-1}.

[1] The two pK_a's of the model compound are comparable to those observed with other porphyrins, ca. 2.3 and 4.0.

Table II: Binding Parameters of Pbiph with Nucleosides and Nucleotides[a]

	λ_{max} Soret (nm)	ε Soret (M^{-1}·cm^{-1})	I/I_0	K (M^{-1})
adenosine	402	7.6×10^4		1.3×10^3
thymidine	401	8.7×10^4	1.00	3.0×10^3
uridine			1.00	
BrdU	403		0.19	9.0×10^2
AMP	402	6.6×10^4	0.90	6.0×10^4
TMP	401	6.6×10^4	0.98	4.0×10^4
CMP			0.98	
GMP			1.00	
dA_4	402		0.78	3.6×10^5
dT_4	402		0.84	9.0×10^4

[a] [Pbiph] = 1–8 μM, cacodylate buffer, pH 6.6, 10 mM NaCl.

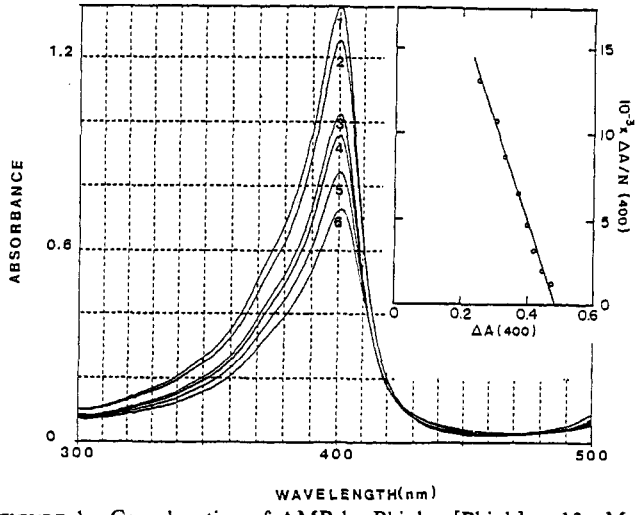

FIGURE 1: Complexation of AMP by Pbiph. [Pbiph] = 13 μM, [NaCl] = 10 mM, cacodylate buffer, pH 6.6, [AMP]/[Pbiph] in phosphate units: 0, 0.4, 2.3, 3.8, 17, 100, numbered 1–6. Inset: plot of $\Delta A/N$ measured at 400 nm versus ΔA. $K = 5.8 \times 10^4$ M^{-1}, using ε{Pbiph free} = 1.02×10^5 M^{-1} cm^{-1}.

Interaction of the Macrotetracycle Pbiph with Small Molecules

1. Nucleosides. The interactions of Pbiph with adenosine, thymidine, and 5-bromodeoxyuridine at pH 6.6 have been studied by absorption and fluorescence spectroscopy. The results are summarized in Table II. The complexation of Pbiph was indicated by a gradual hypochromism of the Soret band as the concentration of nucleoside increased from 0.1 to 50 mM. The absorption spectrum of the complexed porphyrin presents only small red shifts of the Soret band (1–3 nm) and a somewhat larger bathochromic displacement of the two lowest lying Q bands (2–4 nm), at the highest nucleoside concentrations. The fluorescence yields of Pbiph complexed to thymidine and bromodeoxyuridine compared to the emission of the free dye are respectively ϕ/ϕ_0 = 1.00 and 0.19. The

lower fluorescence yield in the case of BrdU results from the heavy-atom effect of the bromine atom. The data fit a simple one-step complexation scheme (eq 2) of the porphyrin Pbiph to the nucleoside N. The binding constants have been de-

$$\text{Pbiph} + \text{N} \overset{K}{\rightleftharpoons} (\text{Pbiph, N}) \qquad (2)$$

termined from the slopes of the graph $\Delta A/[\text{N}]$ versus ΔA, ΔA represents absorbance changes observed at the nucleoside concentration [N] (Lianos & Georghiou, 1979). Binding constants of 900, 3000, and 1300 M^{-1} have been obtained for BrdU, thymidine, and adenosine, respectively. The lower value observed for BrdU compared to thymidine may be due to steric hindrance effects. A binding constant of 670 M^{-1} has been reported for the complexation of the neutral adenine molecule by the tetracationic porphyrin TMPyP (Pasternack et al., 1983).

2. Nucleotides. The complexation of the mononucleotides AMP and TMP and of the oligomers dA_4 and dT_4 haws been studied at pH 6.6, 10 mM NaCl, by absorption and fluorescence methods. The spectrocopic changes observed with nucleotides and nucleosides show similar trends, in the concentration range 0.01–2 mM (Table II). A typical absorption titration curve for the binding of Pbiph to AMP is presented in Figure 1. Small red shifts of the Soret band (1–2 nm) are observed together with a marked hypochromism, larger than that observed with nucleosides. The lowest lying Q band is red-shifted upon binding, from 612 to 615, from 620 to 624 nm in the presence of respectively adenine, AMP, and dA_4. The fluorescence spectra also present a 4-nm red shift, peaking at 623 and 684 nm. The extrapolated fluorescence yield at high ratio of nucleotide/Pbiph (Nc/Pbiph) for AMP, TMP, dA_4, and dT_4 are respectively 0.90, 0.98, 0.78, and 0.84. The fluorescence of the porphyrin bound to CMP and GMP (2 mM) shows no quenching compared to the free dye. The results can be quantified according to a one-step complexation (eq 2), as for the nucleosides. This approach is an approximation in the case of the oligomers. The binding constants obtained for the complexation of Pbiph to AMP, TMP, dA_4, and dT_4 are respectively $(6.0 \pm 1.5) \times 10^4$, $(4.0 \pm 0.8) \times 10^4$, $(3.6 \pm 0.6) \times 10^5$, and $(9.0 \pm 1.5) \times 10^4$ M^{-1}. Comparison of the values obtained for nucleosides and mononucleotides shows an increase of about 40-fold. This difference emphasizes electrostatic effects on the binding constants. A smaller increase in binding affinity is observed between mono- and tetranucleotides, especially in the case of thymidine nucleotides. This different behavior may reflect the difference in oligomer structure: purinic nucleotides are known to stack much better than their pyrimidinic analogues. Thus, the hydrophobic interactions should be larger in the case of oligopurines and may affect the binding constants. The binding constants for Pbiph with AMP and TMP are higher than those reported for TMPyP(4) with mononucleotides and 9,10-anthraquinone sulfonate (Pasternack et al., 1983; Kano et al., 1987). This may be a result of stronger electrostatic and hydrophobic effects of these ligands with Pbiph than with TMPyP(4).

Interaction of Pbiph with Nucleic Acids

1. Absorption Spectra. The interactions of Pbiph with single- and double-stranded polynucleotides have been studied by absorption measurements. A typical titration is shown in Figure 2, for the binding of Pbiph to poly[d(A-T)], in 10 mM NaCl and cacodylate buffer, pH 6.6, at 20 °C. It presents two steps, occurring at different [polynucleotide]/[Pbiph], pNc/Pbiph, ratios: In the first step, observed for low pNc/Pbiph ≤ 1.5, the absorbance in the Soret band decreases and becomes broader with a marked shoulder around 377 nm; an

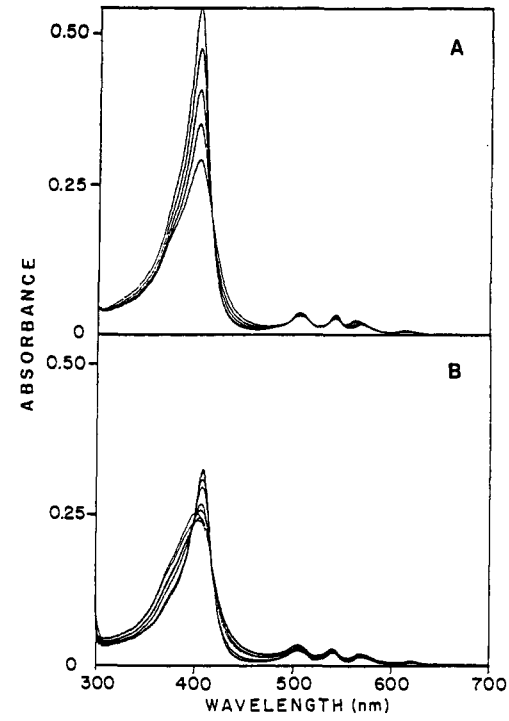

FIGURE 2: Absorption titration of Pbiph with poly[d(A-T)]. [Pbiph] = 5.7 μM, [NaCl] = 10 mM, cacodylate buffer, pH 6.6. (A) pNc/Pbiph in phosphate units from 0 to 0.8; (B) pNc/Pbiph from 4 to 100.

isosbestic point is seen at 412 nm. In the second step, observed for pNc/Pbiph ≥ 2.0, the Soret band and the two lower lying Q bands are red-shifted to 407, 567, and 621 nm, respectively; isosbestic points are observed at 397 and 415 nm.

The binding of Pbiph to other polynucleotides, poly[d-($A^{-5}BrU$)], poly(dA)–poly(dT), and poly[d(G-C)], presents features similar to those described above. In the case of poly[d(G-C)], the Soret band is slightly blue-shifted by 1.5 nm in the pNc/Pbiph range 1.0–2.0 and a clear should is present at 375 nm. The absorption of Pbiph bound to poly(dA) and poly(dT) differs mainly by lower extinction coefficients of the Soret band, compared to A-T double-stranded polynucleotides, and by larger half-bandwidth of the Soret, 3300–4300 cm^{-1} for ss, relative to 1600–1800 cm^{-1} for ds polymers, as can be seen from Figure 3. Comparison of Pbiph binding to nucleotides and polynucleotides shows that only one step is observed for the former, whereas two steps are distinguished in the latter.

2. Emission Spectra. A typical fluorometric titration curve of Pbiph by poly[d(A-T)] at pH 6.6 is shown in Figure 4. Two steps are observed. In the first one, for low pNc/Pbiph (≤2), there is a strong quenching of the dye fluorescence; the relative intensity of the two maxima of free Pbiph, i.e., 618 and 680 nm, decreases and a new vibronic band is formed, peaking at 662 nm. An apparent minimum of the fluorometric titration curve is observed at pNc/Pbiph = 2. A second step occurs at higher pNc/Pbiph. The fluorescence yield of Pbiph is increased with increasing polynucleotide concentration. The fluorescence spectrum is modified: the intensity of the vibronic band at 662 nm decreases, and two vibronic bands appear at 625 and 688 nm, red-shifted by 7–8 nm, compared to free dye. The emission yield of this complex is $\phi/\phi_0 = 1.05 \pm 0.05$ compared to free Pbiph. The comparison of the yield of Pbiph bound to various ds and ss polynucleotides is presented in Table III and Figure 5. The fluorescence yield of Pbiph bound to poly(dA) and poly(dT), at high pNc/Pbiph, is lower than that with poly[d(A-T)]. When the thymine 5-methyl group of

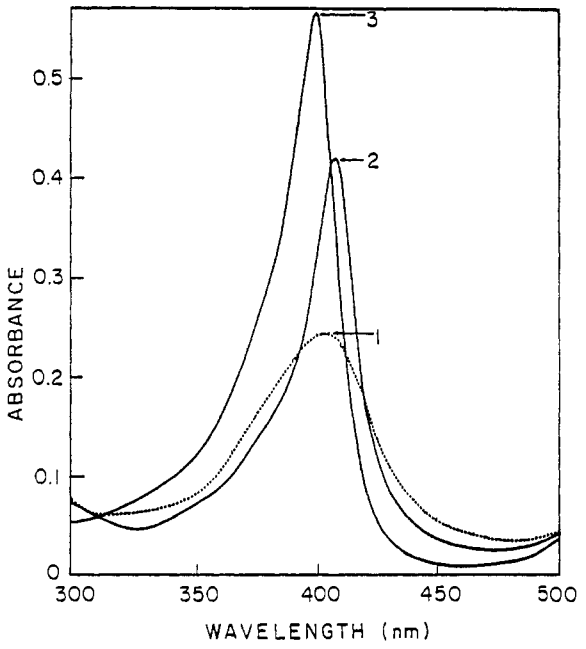

FIGURE 3: Comparison of the absorption spectra of Pbiph free and bound to poly[d(A-T)] and poly(dT). [Pbiph] = 5.6 μM, [NaCl] = 10 mM, cacodylate buffer, pH 6.6. (1) With poly(dT) dashed line; (2) with poly[d(A-T)]; (3) free.

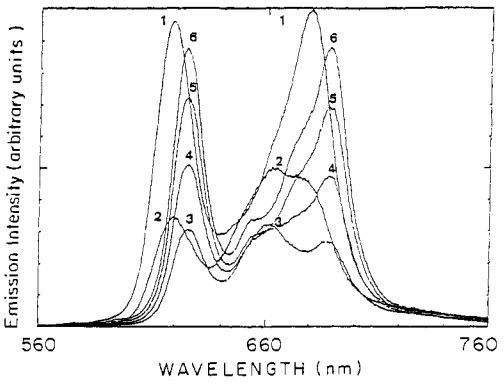

FIGURE 4: Fluorometric titration of Pbiph with poly[d(A-T)]. [Pbiph] = 5.7 μM, [NaCl] = 10 mM, cacodylate buffer, pH 6.6; pNc/Pbiph: 0, 0.9, 1.9, 4.9, 6.5, 50, numbered 1–6.

Table III: Spectroscopic Data of Pbiph Bound to Various Polynucleotides[a]

polymer	λ_{max} (nm) absorption	$\epsilon(\lambda_{max})$ ($M^{-1}\cdot cm^{-1}$)	λ (nm) emission	ϕ/ϕ_0
poly[d(A-T)]	407	6.7×10^4	625, 688	1.05
poly[d(G-C)]	405	5.4×10^4	625, 688	0.71
poly[d(A-^{5}BrU)]	408	6.6×10^4	625, 688	0.59
poly(dT)	403	5.0×10^4	626, 687	0.75
poly(dA)	405	5.3×10^4	623, 685	0.37

[a] pH 6.6, cacodylate buffer (10 mM).

poly[d(A-T)] is replaced by a bromine atom, i.e., poly[d(A-^{5}BrU)], the Pbiph fluorescence is quenched, $\phi/\phi_0 = 0.59 \pm 0.03$. This quenching by poly[d(A^{-5}BrU)] is larger at lower ionic strength, $\phi/\phi_0 = 0.27$ at 3 mM NaCl. The bromine atom of poly[d(A-^{5}BrU)], quenches Pbiph fluorescence mainly by static interactions as will be seen from the lifetime measurements. Since poly[d(A-^{5}BrU)] quenching can be compared to that of BrdU and since its Br atom protrudes into the major groove, the location of the porphyrin ring may be close to or in the major groove. The fluorescence of Pbiph bound to poly[d(G-C)] is quenched relative to that of poly[d(A-T)]. This is also the case with other cationic porphyrins like H_2TMPyP(4) (Kelly & Murphy, 1985).

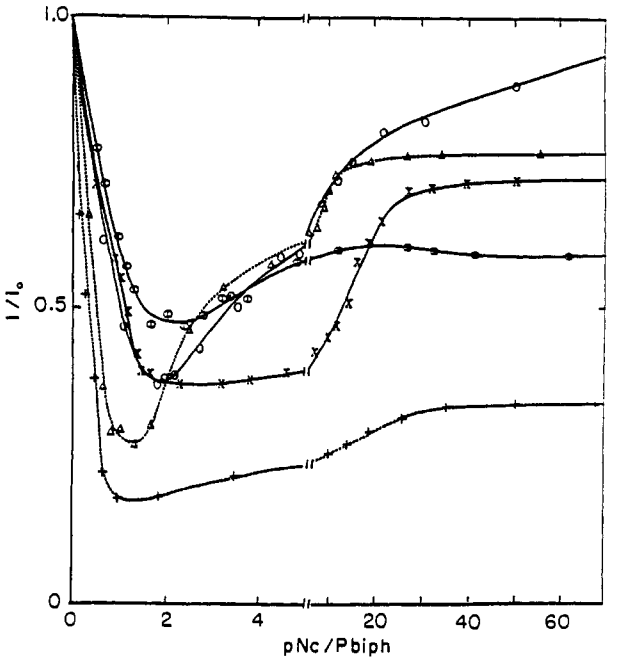

FIGURE 5: Comparison of fluorometric titration of Pbiph with various polynucleotides. Excitation wavelength at 410 nm. The data are corrected for changes in absorbance at the excitation and for dilution. It represents the integrated fluorescence spectra in the presence of polymer normalized to the emission of free Pbiph. [Pbiph] = 5–7 μM, [NaCl] = 10 mM, cacodylate buffer, pH 6.6. (O) Poly[d(A-T)], (⊖) poly[d(A-^{5}BrU)], (X) poly[d(G-C)], (+) poly(dA), (Δ) poly(dT).

3. Emission Lifetimes. Table IV summarizes typical experiments with aerated solutions of Pbiph in the absence and in the presence of various polynucleotides at pH 6.6.

(*a*) *Free Pbiph.* Best fits of the experimental points were obtained by two exponential components of the form

$$F(t) = A + \sum_{i=1}^{n} B_i \exp(-t/\tau_i)$$

where τ_i represents the lifetime of the ith component and B_i its relative weight: $\tau_1 = 16.1 \pm 0.1$ ns, $B_1 = 90\%$, and $\tau_2 = 7 \pm 1$ ns, $B_2 = 10\%$.

(*b*) *Binding of Pbiph to Poly[d(A-T)], Poly[d(A-^{5}BrU)], and Poly[d(G-C)].* The fluorescence decays, at high pNc/Pbiph, are best fitted by two exponential components. The first one has a somewhat longer lifetime in the presence of poly[d(A-T)] and poly[d(G-C)] than the free dye $\tau_1 = 17$–18 ns. The second component has a shorter lifetime than free Pbiph, $\tau_2 = 3.9$–5.2 ns, although it is not very accurately defined. The longest lifetime is shorter with poly[d(A-^{5}BrU)] than with poly[d(A-T)], $\tau_1 = 15.4 \pm 0.1$ ns. This dynamic quenching accounts only partly for the low fluorescence yield of Pbiph complexed to poly[d(A^{-5}BrU)], observed by steady-state measurements. Thus a large contribution to the quenching is static.

A very short component is observed at low pNc/Pbiph and its lifetime depends on this ratio. Its weight decreases with increasing pNc/Pbiph. It is observed at both 10 and 100 mM NaCl. Since dimers of porphyrin are known to be nonfluorescent (Brault et al., 1986), the shortest component may be attributed to Pbiph molecules aggregated along poly[d(A-T)], which acts as a polyelectrolyte. Since the electrostatic interaction between negatively charged polynucleotide and positively charged Pbiph is increased at lower ionic concentration, more aggregation is expected.

(*c*) *Lifetime of Pbiph Bound to Poly(dT) and Poly(dA).* The fluorescence decays, at low pNc/Pbiph, are best fitted by three components. The shortest one, $\tau_3 = 0.6$–0.9 ns, whose

Table IV: Lifetimes of Pbiph in the Presence of Various Polynucleotides[a]

entry	polymer	pNc/Pbiph	τ_1 (ns)	B_1 (%)	τ_2 (ns)	B_2 (%)	τ_3 (ns)	B_3 (%)	χ^2	DW
1	none		16.1 ± 0.1	90	7.4 ± 0.6	10			1.12	1.90
2	poly[d(A-T)]	7	18.0 ± 0.1	3	8.2 ± 0.4	1	0.10 ± 0.02	96	1.08	2.06
3		40	18.07 ± 0.06	52	7.3 ± 0.1	29	1.28 ± 0.09	19	1.09	1.73
4		80	17.9 ± 0.1	75	6.5 ± 0.2	25			1.21	1.80
5		200	17.9 ± 0.1	90	5.2 ± 0.2	10			1.22	1.65
6	poly[d(A-^{5}BrU)]	80	15.4 ± 0.1	65	5.4 ± 0.2	35			1.38	1.67
7	poly[d(G-C)]	10	17.8 ± 0.1	12	6.2 ± 0.1	56	2.3 ± 0.1	32	0.93	1.89
8		100	17.0 ± 0.2	30	3.9 ± 0.6	70			1.19	1.71
9	poly(dT)	40	18.1 ± 0.2	41	8.2 ± 0.2	33	0.88 ± 0.15	26	1.32	1.81
10		80	18.7 ± 0.1	64	11.7 ± 1.0	19	0.90 ± 0.10	17	1.12	1.73
11	poly(dA)	20	16.22 ± 0.05	4	4.5 ± 0.1	15	0.59 ± 0.04	81	1.33	1.84
12	*b*	90	15.8 ± 0.2	34	3.6 ± 0.4	66				
13	poly[d(A-T)][c]	14	18.15 ± 0.05	20	5.9 ± 0.5	38	2.4 ± 0.2	42	1.24	
14		80	17.97 ± 0.05	74	7.0 ± 0.5	26			1.06	1.74
15		200	17.97 ± 0.05	84	5.1 ± 0.5	16			1.06	

[a] Excitation at 350–420 nm, single photon counting experiments, pH 6.6, 10 mM NaCl, in air-saturated solutions. [b] Nitrogen laser excitation with a 1-ns pulse, at 337 nm. [c] 100 mM NaCl, 10 mM cacodylate buffer.

weight decreases with increasing pNc/Pbiph, is attributed to aggregates as above. The longest lifetime of Pbiph bound to poly(dT) is comparable to that observed with poly[d(A-T)], whereas it is shorter in the case of poly(dA).

(*d*) *Lifetimes in a Mixture of Single- and Double-Stranded Polymers.* The lifetime of Pbiph in the presence of poly(dA) and poly[d(A-T)] in a molar ratio of 1/1, with a 90-fold excess of polymers over Pbiph was measured in order to investigate ss/ds binding selectivity. The following lifetimes have been observed: poly(dA), τ_1 = 15.8 ± 0.2 ns (34%), τ_2 = 3.6 ± 0.4 ns (66%); poly[d(A-T)], τ_1 = 18.7 ± 0.2 ns (92%), τ_2 = 5.0 ± 0.6 ns (8%); 1/1 mixture, τ_1 = 15.9 ± 0.2 ns (38%), τ_2 = 3.7 ± 0.4 ns (62%). These results are consistent with a preferential binding of Pbiph to ss poly(dA) in a 1/1 mixture with ds poly[d(A-T)].

4. Binding Constants. The absorption and fluorometric titrations presented above show two steps in the binding of Pbiph to polynucleotides. The first one is a DNA-induced self-association by stacking of the dye along the DNA polyanion. The second binding step, observed with increasing polymer concentration, represents the binding of Pbiph to isolated sites on the polynucleotide. The aggregation is observed in the range of ionic concentrations studied, 1–100 mM NaCl. The hypochromism and fluorescence quenching are more pronounced in the low ionic concentration range, as a result of stronger electrostatic interactions between negatively charged polynucleotide and positively charged Pbiph. The conversion of aggregated to isolated sites is more efficient at low ionic concentration.

Since the first step could not be abolished under any experimental condition and the sharp decrease of the fluorescence at low pNc/Pbiph indicates a strong binding (Figure 5), the binding constants for this step could not be calculated. Using light scattering measurements as a criterion of separation between the two steps, (Kapuscinski & Darynkiewicz, 1987), we attempted to calculate the binding constants of the second step, using Scatchard analysis (Scatchard, 1949).

Table V: Binding Constants of Pbiph to Polynucleotides[a]

polymers	pH 6.6 K (M^{-1})	pH 6.6 n	pH 4.6 K (M^{-1})	pH 4.6 n
poly(dA)	1×10^6	4.0	3×10^6	10.0
poly(dT)	6×10^5	2.0		
poly[d(A-T)]	9×10^4	4.0	1×10^5	3.5
poly(dA)–poly(dT)	2×10^5	5.5	9×10^4	5.0
poly[d(G-C)]	2×10^5	4.0		

[a] Obtained from Scatchard plots of ν/L, where ν is the binding density, n is the exclusion site (maximal number of Pbiph per base pair), and L the concentration of Pbiph aggregates formed during the first complexation step. Those parts of the fluorimetric titration curves were used where the light scattering of Pbiph polynucleotides solutions was similar to that of free polymer ones at 10 mM NaCl, [Pbiph] = 0.6–9 μM.

$$(\text{Pbiph, pNc})_{\text{aggregates}} \overset{\text{pNc}}{\rightleftharpoons} (\text{Pbiph, pNc})_{\text{isolated}} \quad (3)$$

The results at pH 6.6 and 4.6, [NaCl] = 10 mM, are presented in Table V. The data show larger binding constant for single-stranded polymers poly(dT) and poly(dA) than for double-stranded ones, especially at low pH, indicating *a selectivity between ss and ds polynucleotides.* At pH 4.6, Pbiph possesses four positive charges, compared to about two at pH 6.6. Although the binding constants for double-stranded polymers increase somewhat, the main effect of lowering the pH is to increase the affinity for single-stranded polynucleotides, suggesting other type(s) of interaction, in addition to the electrostatic one. The change of the exclusion site with pH in the presence of only ss poly(dA), from 4.0 base pairs at pH 6.6 to 10.0 base pairs at pH 4.6, may hint at the effect of a larger flexibility of this polymer at low pH. The exclusion

site for ds polymers at both pHs is 4.4 base pairs, which corresponds to an average distance of c.a. 14.5 Å between Pbiph units, assuming no distortion of the double helix and a random nonselective distribution.

The binding constants of Pbiph for poly[d(A-T)] and poly(dA)-poly(dT) are comparable, which differs markedly from binding of known intercalators. Intercalating drugs bind more tightly to poly[d(A-T)] than to poly(dA)-poly(dT) (Wilson et al., 1985). This difference in affinity is attributed to the peculiar structure of the latter polymer, characterized by a large propeller twist and bifurcated H bonds, which prevents an easy intercalation (Nelson et al., 1987). Therefore, the similarity of the binding constants with alternated and nonalternated A-T polynucleotides shown by Pbiph may be taken as *indicative of nonintercalation.*

The binding affinity of Pbiph for the alternated GC polymer is slightly higher than for AT. Whereas H_2TMPyP(4) shows similar affinities for poly[d(A-T)] and poly[d(G-C)], ZnTMPyP(4) binds about 200 times more strongly to AT sites than to GC sites (Pasternack et al., 1983; Kelly & Murphy, 1985; Strickland et al., 1988). This preferential binding to AT sites has been suggested to result from conformational distortion that permits a better charge interaction of ZnTMPyP(4) with AT than with GC polymers.

5. Competition Experiments. Competition experiments have been performed in order to evaluate the binding constant of Pbiph to poly[d(A-T)]. 4′,6-Diamidino-2-phenylindole, DAPI, bound to poly[d(A-T)], pNc/[DAPI] = 100, is displaced by excess Pbiph ([Pbiph]/[DAPI] = 1–10). This results from the shift of DAPI excitation maximum from 360 to 341 nm, which correspond to bound and free DAPI, respectively (fluorescence monitored at 455 nm), and from the decrease of its fluorescence intensity. In parallel, a shift of the excitation maximum of Pbiph from 400 to 408 nm is observed (emission measured at 688 nm). The binding constant of DAPI alone to poly[d(A-T)], at pH 6.6, 10 mM NaCl, obtained by Scatchard analysis, $K_1 = 2 \times 10^7$ M^{-1}, is compatible with the value reported by Manzini et al. (Manzini et al., 1985). The binding constant of Pbiph to poly[d(A-T)], $K_2 = 6 \times 10^4$ M^{-1}, $n_2 = 6$, calculated from the competition experiments, is in agreement with the Scatchard analysis for the binding Pbiph to poly[d(A-T)] presented above.

6. Fluorescence Anisotropy. Fluorescence polarization techniques have been used to monitor the motion of dyes complexed with DNA and also to study internal and overall motions of DNAs of various length and sequence (Haerd & Kearns, 1986). If the dye is "rigidly" bound to DNA, like in an intercalation site, its rotational mobility is reduced and it may be compared to immobilized dye polarization (in viscous solvent and/or at low temperature). Anisotropic motions of fluorescent dyes can be monitored by studying the polarization anisotropy resulting from different excitation wavelengths. If the absorption transition moments of two electronic transitions have different polarization directions within the molecule, then the anisotropic motions will contribute differently to their depolarization. The fluorescence polarization anisotropy, r, is defined as

$$r = (I_{\parallel} - I_{\perp})/(I_{\parallel} + 2I_{\perp}) \quad (4)$$

where I is the fluorescence intensity and the subscripts indicate that it is observed parallel or perpendicular to the polarization of the exciting light.

a. Pbiph in Glycerol. The absorption and fluorescence spectra of Pbiph in 90% glycerol have been recorded at 0.8 ± 0.2 °C. The Soret band and the two lowest lying Q bands are red-shifted respectively to 404, 563, and 615 nm, compared

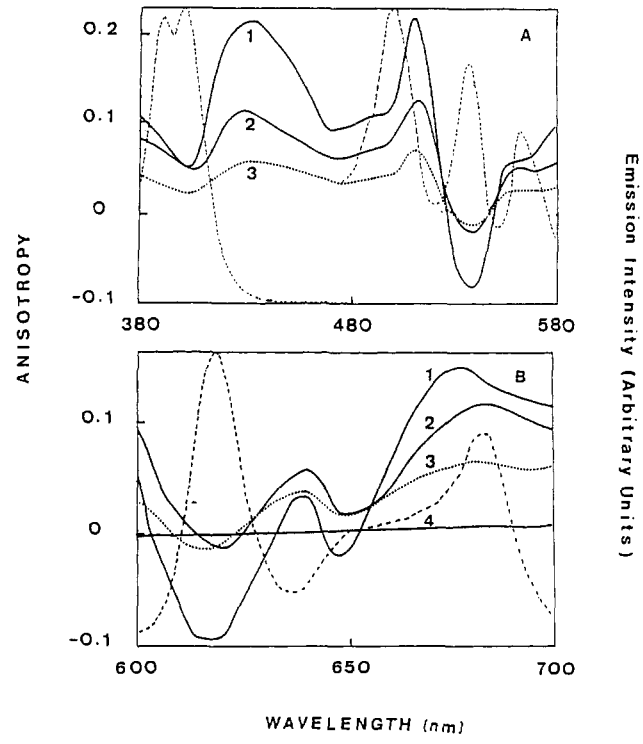

FIGURE 6: Fluorescence anisotropy of Pbiph in 90% glycerol (1) and in poly[d(A-T)] (2) and poly(dT) (3) (pNc/Pbiph = 100), in buffer solution (4), [NaCl] = 10 mM, cacodylate buffer, pH 6.6. (A) Excitation anisotropy spectra, emission monitored at 620 nm (left scale). Dashed line (fluorescence intensity scale, arbitrary units): excitation spectrum of Pbiph in 90% glycerol, fluorescence measured at 620 nm. The Q-band scale is 28-fold more extended than the Soret scale. (B) Emission anisotropy spectra; excitation at 537 nm (1), 547 nm (2), and 538 nm (3) (left scale). Dashed line (right scale) (fluorescence intensity scale, arbitrary units): fluorescence spectrum of Pbiph in 90% glycerol, excitation at 400 nm.

to water. The excitation spectrum shows a splitting of the Soret band into two vibronic bands at 392 and 401 nm (Figure 6A). The fluorescence spectrum is modified compared to that in water solutions: in addition to the two bands at 619 and 683 nm, a marked shoulder is observed at 655 nm. The excitation fluorescence anisotropy spectrum, monitored at 620 nm, is presented in Figure 6A. Maxima are observed at 432 and 511 nm, minima at 402 and 539 nm. Broad shoulders are seen around 480 and 557 nm. No fluorescence anisotropy is present in glycerol-free aqueous solutions at the same temperature.

These results may be interpreted by analogy to anisotropy spectra of pheophytin and Coporphyrin II tetramethyl ester (Gouterman & Stryer, 1962; Weiss, 1972). The well-resolved peaks at 539 and 511 nm are attributed to $Q_y(1 \leftarrow 0)$ and $Q_y(0 \leftarrow 0)$ transitions, respectively. The broad shoulder at 557 nm corresponds to the second $Q_x(1 \leftarrow 0)$ transition, whereas the first $Q_x(0 \leftarrow 0)$ band is observed as a positive peak at about 612 nm. The "split" Soret anisotropy, peaking at 402 nm, is apparently only weakly x polarized. Its red edge seems y polarized relative to the main peak. The results obtained for Pbiph are consistent with those reported for various free-base porphyrins at low temperature (Gouterman & Stryer, 1962; Baer et al., 1961).

b. Pbiph Bound to Polynucleotides. The excitation anisotropy spectra of Pbiph bound to poly[d(A-T)] and to poly(dT) are shown in Figure 6A. The porphyrin fluorescence is less polarized than in glycerol, even at high pNc/Pbiph ratios. The anisotropy at 511 nm, $Q_y(1 \leftarrow 0)$ transition, is 0.135 in the presence of poly[d(A-T)], compared to 0.221 in polymer-free glycerol solutions. It is also reduced in the $Q_y(0$

← 0) transition at 539 nm, to −0.018 compared to −0.083 in glycerol. A greater decrease of the (0 ← 0) emission vibronic band compared to the (1 ← 0) one is clearly observed in Figure 6B. The anisotropy in the Q_x(1 ← 0) transition at 560 nm observed in the presence of poly[d(A-T)] (0.054) differs slightly from that found in glycerol (0.060) (Figure 6A). The *y*-polarized transition at 430 nm presents a lower anisotropy value in the presence of poly[d(A-T)] than in glycerol, whereas no change is observed at 402 nm. The same trend is observed for Pbiph bound to poly(dT), and the extent of anisotropy is lower than with poly[d(A-T)].

c. Discussion. In the complexation of Pbiph to polynucleotides, we have to assume that the porphyrin symmetry remains unchanged upon binding and that polarization data may be evaluated in terms of anisotropic motions (Haerd & Kearns, 1986). This assumption may be justified on the basis of symmetry changes observed in substituted porphyrin. When symmetry axes are lost in porphyrins derivatives, the (0 ← 0) emission and absorption bands exhibit high polarization compared to (1 ← 0) ones. The (0 ← 0) emission band is clearly less polarized than the (1 ← 0) band (Figure 6B). The (0 ← 0) Q_y absorption band (excitation) has also a relatively more reduced anisotropy, compared to the (1 ← 0) Q_y band (Figure 6A). Therefore, a decrease of symmetry due the binding of Pbiph to DNA seems unlikely.

Any transfer of excitation energy from DNA bases to the dye would lead to depolarization of the light emitted from the dye. No significant energy transfer has been observed in these conditions.

The results presented are consistent with the reduction of the rotational freedom of the porphyrin ring by steric effects. Steric effects have been invoked in order to explain the larger polarization of ethidium bromide and of the bis-intercalator bis(9-aminoacridinyl)pyrazole compared to 9-aminoacridine intercalated into DNA (Haerd & Kearns, 1986). Pbiph is bound to poly[d(A-T)] by strong electrostatic attraction of the positively charged ammonium groups of the lateral rings to the negatively charged polymer. The thermal denaturation results (see below), and the similar bonding constants observed with alternated and nonalternated A-T polymers, suggest that Pbiph is unable to intercalate like planar aromatic cations, in accordance with its bulky structure. Therefore, Pbiph may be located in one of the grooves. This assumption is consistent with the red shifts observed in absorption and fluorescence. If Pbiph were located in the minor groove, which is not large enough to include all of it, its rotational freedom should be large, resulting in a pronounced decrease of the fluorescence anisotropy, compared to that observed in glycerol. If Pbiph were located in the major groove, in which the whole molecule can fit, the rotational mobility of the porphyrin should be significantly reduced, and therefore a relatively large anisotropy is expected. This location is also consistent with the fluorescence quenching by the poly[d(A-^{5}BrU)] bromine atom, which protrudes into the major groove. Therefore, the results suggest *that the binding site of Pbiph could be the major groove.*

Comparison of anisotropy spectra of Pbiph bound to poly[d(A-T)] and in glycerol shows a larger decrease in the *y*-polarized visible bands, i.e., 512 nm and 547 nm (respectively 39% and 78%), than in the *x*-polarized band at 560 nm, where only a 10% decrease is observed. The large variation in *y*-polarized bands, observed upon binding to polynucleotide, may be attributed to a larger rotational freedom of the porphyrin ring along the *y* axis than along the *x* axis. The crystal structure of the Cu(II) complex of Pbiph (B. Chevrier and D. Moras, unpublished results) shows a tilting of the macrocycle cages, which could be related to the present photophysical observations.

Table VI: Thermal Denaturation of Poly[d(A-T)] in the Presence of Pbiph[a]

[Pbiph] (μM)	T_m(260 nm) ± 1 °C	T_m(406 nm) ± 1 °C
0	44.0	
1.6	44.4	45.6
4.0	45.0	46.8
8.0	47.8	47.6

[a] [poly[d(A-T)] = 160 μM, pH 6.6, 10 mM NaCl.

The lower polarization of Pbiph bound to poly(dT), compared to poly[d(A-T)] (pH 6.6), is compatible with a less "tight" binding site, in which its rotational mobility is much higher.

7. Thermal Denaturation. The thermal stability of poly[d(A-T)] in the presence and absence of Pbiph has been measured in 10 mM NaCl and 1 mM cacodylate buffer, pH 6.6. Typical results are presented in Table VI. The thermal denaturation of poly[d(A-T)] is observed at 44.4 ± 0.1 °C. The transition from double strand to single strand has been monitored in the presence of Pbiph, at pNc/Pbiph = 40 and 100, where the absorbance changes at 260 nm upon increasing temperature are very similar to that observed in polymer-free solutions. Only at the highest Pbiph concentration, pNc/Pbiph = 20, is T_m shifted by 3.7 °C to 47.8 ± 0.1 °C, and the transition becomes slightly less cooperative. The absorbance changes have also been measured at 407 and 400 nm, which are respectively the maxima of bound and free Pbiph. When the temperature is raised from 20 to 55 °C, a large decrease of the absorption at 407 nm is observed, whereas at 400 nm, it decreases only by 8%. The absorption spectra measured at 55 °C show a blue shift and broadening of the Soret band, whereas two Q bands at 504 and 565 nm are red-shifted compared to the spectrum at 20 °C.[2] The comparison of T_m values calculated from absorption data at 260 and 407 nm shows that the latter are slightly higher than the former.

The results enable us to draw the following qualitative conclusions:

(1) There is no significant stabilization of the double helix upon binding of Pbiph, since only small T_m shifts have been observed. This lack of ds stabilization is consistent with a *nonintercalation of Pbiph in double-stranded polynucleotide*, since intercalators are known to stabilize it strongly, by shifting the ds/ss transition to higher temperature (Asseline et al., 1984).

(2) The large decrease of absorption at 407 nm, upon increasing the temperature, while there is no parallel increase but rather a small decrease at 400 nm, is attributed to the *preferential binding of Pbiph to denaturated poly[d(A-T)]*. If Pbiph were released in the bulk as the polynucleotide is denaturated, an increase of the absorbance should be observed at 400 nm, the absorption maximum of free Pbiph. This is not observed. From isotherm binding curves, the extinction coefficients of Pbiph bound to poly[d(A-T)], poly(dA), and poly(dT) have been calculated. They are higher at 407 nm in the presence of double-stranded than in the presence of single-stranded polymers: $\epsilon = 6.7 \times 10^4$ M^{-1} cm^{-1} in the presence of poly[d(A-T)] and $(4.9–5.1) \times 10^4$ M^{-1} cm^{-1} with poly(dA) and poly(dT). The decrease of absorbance at 407 nm (assuming similar extinction coefficients at 20 and 55 °C)

[2] Pbiph polymer-free solutions show an absorbance decrease of 18% in the heating–cooling cycles between 20 and 55 °C. This is not observed when Phiph is bound to poly[d(A-T)].

and the change in absorption spectra at 55 °C are consistent with increasing binding to Pbiph to single-stranded polymer with raising temperature.

(3) The somewhat different T_m, obtained when measured in the polymer and Pbiph Soret maxima, might be due to the formation of single-stranded domains, followed by the preferential binding of Pbiph in these denaturated regions.

Conclusion

The binding of Pbiph to polynucleotides occurs in two steps: the first one is a highly cooperative binding of Pbiph aggregates along the polymer; the second one is the binding of Pbiph to isolated sites. The data on the affinity of Pbiph for isolated sites on ss and ds polymers indicate that *Pbiph is more strongly bound to single-stranded than to double-stranded polynucleotides*. Thermal denaturation experiments show that Pbiph binds efficiently to denaturated DNA and does not stabilize the double-helical structure. The highest affinity at pH 6.6 has been found for poly(dA). The results at pH 4.6 indicate a larger ss/ds selectivity than at pH 6.6. The greater charge of Pbiph at lower pH and the flexibility of single-stranded polynucleotides for the binding of the bulky Pbiph molecule, compared to the double-helix structure, could account for the selectivity observed. It seems that the Pbiph molecule has larger rotational "freedom" in ss than in ds polymers, as the fluorescence anisotropy results indicate. On this basis, it may be suggested that selective ss binding molecules should possess sterically hindered structures and should be highly positively charged.

The similarity between the binding constants of Pbiph to poly[d(A-T)] and poly(dA)-poly(dT) and the very small stabilization of the double helix observed in the melting experiments are in agreement with of a nonintercalative binding site of this dye in double-stranded polynucleotides. This assumption is also consistent with the bulky structure of the Pbiph molecule and with the nonintercalation reported for Zn(II), Co(II), Fe(III), and Mn(III) metalloporphyrins bearing axial ligands, on the basis of steric requirements imposed by these axial ligands (Gibbs et al., 1988). ZnTMPyP(4) has been suggested to bind along the minor groove of AT regions, probably as a two- or three-charge interaction, producing cooperative conformational changes in DNA structure (Strickland et al., 1988). Molecules bound in the DNA minor groove, like netropsin and ZnTMPyP, present a marked selectivity for A-T sites (Wartell et al., 1974). This is not observed with Pbiph. Fluorescence anisotropy results, together with the fluorescence quenching by the bromine atom of poly[d(A-^{5}BrU)], suggest a *location of Pbiph into the major groove* (Dattagupta et al., 1980; Coll et al., 1989).

Both characteristic features, (1) *binding selectivity* with preference for ss over ds polynucleotides and (2) *binding location*, preference for the major groove, may be considered to result from the *macrocyclic cryptand cage structure* into which the porphyrin unit is incorporated. These two properties may respectively be related to the steric hindrance to intercalative insertion of the porphyrin ring due to the rigidity of the cage walls and the overall bulk of the molecule. The flexibility/rigidity of the linkers seems to play an important role in the ability of macrocyclic molecules to intercalate into DNA, as suggested by the bis-intercalation (Zimmerman et al., 1989) observed in a macrocyclic bisacridine.

By extension and using the same principles, it should be possible to design other nucleic acid probes showing ss/ds and/or major groove/minor groove selectivity; this may in particular be the case for macrocyclic (Lehn et al., 1988) and macrobicyclic (Claude et al., 1989) bis-intercalators containing intercalating heterocyclic groups (phenazine, acridines).

Acknowledgments

We thank Professor Claude Hélène, Dr. Michel Rougée, and Dr. Thérèse Montenay-Garestier (Muséum d'Histoire Naturelle) and Professor Michael Ottolenghi (The Hebrew University of Jerusalem) for the use of photophysical equipment and Dr. A. J. Blacker for a sample of the model compound as well as the Ministère des Affaires Etrangères for a postdoctoral fellowship to A.S.S.

Registry No. Pbiph, 90633-79-7; BrdU, 59-14-3; AMP, 61-19-8; TMP, 365-07-1; CMP, 63-37-6; GMP, 85-32-5; dA_4, 68726-43-2; dT_4, 2476-57-5; poly[d(A-^{5}BrU)], 53079-00-8; poly(dA)-poly(dT), 24939-09-1; poly[d(A-T)], 28677-60-3; poly(dT), 25086-81-1; poly[d(G-C)], 95754-57-7; poly(dA), 25191-20-2; adenosine, 58-61-7; thymidine, 50-89-5.

References

Asseline, U., Delarue, M., Lancelot, G., Toulme, F., Thuong, N., Montenay-Garestier, T., & Hélène, C. (1984) *Proc. Natl. Acad. Sci. U.S.A. 81*, 3297–3301.

Baer, F., Lang, H., Schnabel, E., & Kuhn, H. (1961) *Z. Elektrochim. 65*, 346–354.

Brault, D., Vever-Bizet, C., & Le Doan, T. (1986a) *Biochim. Biophys. Acta 857*, 238–250.

Brault, D., Vever-Bizet, C., & Dellinger, M. (1986b) *Biochimie 68*, 913–921 and references cited therein.

Bromley, S. D., Ward, B. W., & Dabrowiak, J. C. (1986) *Nucleic Acids Res. 14*, 9133–9148.

Carvlin, M. J., & Fiel, R. J. (1983) *Nucleic Acids Res. 11*, 6121–6139.

Chow, Y. F. A., Dolphin, D., Paine, J. P., III, McGarvey, D., Pottier, R., & Truscott, T. G. (1988) *J. Photochem. Photobiol. B 2*, 253–263.

Claude, S., Lehn, J.-M., & Vigneron, J.-P. (1989) *Tetrahedron Lett. 30*, 941–944.

Coll, M., Aymami, J., van der Marel, G. A., van Boom, J. H., Rich, A., & Wang, A. H.-J. (1989) *Biochemistry 28*, 310–320.

Dattagupta, N., Hogan, M.,& Crothers, D. M. (1980) *Biochemistry 19*, 5998–6005.

Dolphin, D., Ed. (1979) *The Porphyrins*, Vol. 3, Chapter 1, pp 33–47, Chapter 7, pp 340–341, Academic Press, New York.

Fiel, R. J., Howard, J. C., Mark, E. H., & Datta Gupta, N. (1979) *Nucleic Acids Res. 6*, 3093–3118.

Ford, K., Fox, K. R., Neidle, S., & Waring, M. J. (1987) *Nucleic Acids Res. 15*, 2221–2234.

Geacintov, N. E., Ibanez, V., Rougée, M., & Bensasson, R. V. (1987) *Biochemistry 26*, 3087–3092.

Gibbs, E. J., Maurer, M. C., Zhang, J. H., Reiff, W. M., Hill, D. T., Malicka-Blaszkiewicz, M., McKinnie, R. E., Liu, H.-Q., & Pasternack, R. (1988) *J. Inorg. Biochem. 32*, 39–65.

Gouterman, M., & Stryer, L. (1962) *J. Chem. Phys. 37*, 2260–2266.

Gubelmann, M., Harriman, A., Lehn, J.-M., & Sessler, J. L. (1988) *J. Chem. Soc., Chem. Commun.*, 77–79.

Haerd, T., & Kearns, D. R. (1986) *J. Phys. Chem. 90*, 3437–3444.

Hamilton, A. D., Lehn, J.-M., & Sessler, J. L. (1984) *J. Chem. Soc., Chem. Commun.*, 311–313.

Hamilton, A. D., Lehn, J.-M., & Sessler, J. L. (1986) *J. Am. Chem. Soc. 108*, 5158–5167.

IUPAC Commission on Photochemistry (1986) *EPA Newsl.*, 21–29.
Kalyanasundaram, K., & Neumann-Spallart, M. (1982) *J. Phys. Chem. 86*, 5163–5169.
Kano, K., Nakajima, T., & Hashimoto, S. (1987) *J. Phys. Chem. 91*, 6614–6619.
Kapuscinski, J., & Darzynkiewicz, Z. (1987) *J. Biomol. Struct. Dyn. 5*, 127–143.
Kelly, J. M., & Murphy, M. J. (1985) *Nucleic Acids Res. 13*, 167–184.
Le Doan, T., Perrouault, L., Hélène, C., Chassignol, M., Thuong, N. T. (1986) *Biochemistry 25*, 6736–6739.
Lehn, J.-M., Schmidt, F., & Vigneron, J.-P. (1988) *Tetrahedron Lett. 29*, 5255–5258.
Lianos, P., & Georghiou, S. (1979) *Photochem. Photobiol. 29*, 13–21.
Lown, J. W., & Joshua, A. V. (1982) *J. Chem. Soc., Chem. Commun.*, 1298–1300.
Malik, Z., & Faraggi, A. (1988) *Book of Abstracts*, 10th International Congress on Photobiology, Jerusalem, Israel, p 11.
Manzini, G., Xodo, L., Barcellona, M. L., & Quadrifoglio, F. (1985) *Proc. Int. Symp. Biomol. Interactions. Suppl. J. Biosci. 8*, 699–711.
Nelson, H. C. M., Finch, J. T., Luisi, B. F., & Klug, A. (1987) *Nature 330*, 221–226.
Pasternack, R. F., Gibbs, E. J., & Villafranca, J. J. (1983a) *Biochemistry 22*, 2406–2414.
Pasternack, R. F., Gibbs, E. J., & Villafranca, J. J. (1983b) *Biochemistry 22*, 5409–5417.
Scatchard, G. (1949) *Ann. N.Y. Acad. Sci. 51*, 660–672.
Strickland, J. A., Marzilli, L. G., Gay, K. M., & Wilson, W. D. (1988) *Biochemistry 27*, 8870–8878.
Ward, B., Skorobogaty, A., & Dabrowiak, J. C. (1986) *Biochemistry 25*, 7827–7833.
Wartell, R. M., Larson, J. E., & Wells, R. D. (1974) *J. Biol. Chem. 249*, 6719–6731.
Weiss, C., Jr. (1972) *J. Mol. Spectrosc. 44*, 37–80.
Wilson, W. D., Wang, Y. H., Krishnamoorthy, C. R., & Smith, J. C. (1985) *Biochemistry 24*, 3991–3999.
Zimmerman, S. C., Lamberson, C. R., Cory, M., & Fairley, T. A. (1989) *J. Am. Chem. Soc. 111*, 6805–6809.

Purification of a Strand Exchange Stimulatory Factor from *Saccharomyces cerevisiae*†

David Norris and Richard Kolodner*

Department of Biological Chemistry and Molecular Pharmacology, Harvard Medical School, Boston, Massachusetts 02115, and Dana-Farber Cancer Institute, 44 Binney Street, Boston, Massachusetts 02115

Received February 21, 1990; Revised Manuscript Received May 17, 1990

ABSTRACT: The SEP1 strand exchange protein of *Saccharomyces cerevisiae* catalyzes the formation of heteroduplex DNA joints between single-strand circles and homologous linear duplexes in vitro. Previous work [Kolodner, R., Evans, D. H., & Morrison, P. T. (1987) *Proc. Natl. Acad. Sci. U.S.A. 84*, 5560–5564] showed that the optimal stoichiometry of SEP1 in this reaction was 1 SEP1 monomer per 12–14 nucleotides of single-stranded DNA. The work presented here describes the purification and characterization of a 33 000-dalton yeast protein that permits SEP1 to catalyze joint molecule formation at much lower stoichiometries. In the presence of this second factor, which has been designated SF1 for *s*timulatory *f*actor *1*, the optimal amount of SEP1 dropped to 1 SEP1 monomer per 725 nucleotides of single-stranded DNA. At this concentration of SEP1, the rate of joint molecule formation increased approximately 3-fold over that seen in the unstimulated reaction (no SF1). Titration experiments indicated that when the concentration of SEP1 was reduced over 300-fold to 1 SEP1 molecule per 5800 nucleotides of single-stranded DNA, the stimulated reaction had the same rate and extent of joint molecule formation as the unstimulated reaction. The optimal amount of SF1 was 1 molecule of SF1 per 20 nucleotides of single-stranded DNA. Electron microscopic analysis showed that a bona fide strand exchange reaction produced the joint molecules in the stimulated reaction. The stimulated reaction had requirements that were essentially identical with those seen in the unstimulated reaction, including a lack of dependence on ATP. SF1 aggregated single-stranded and double-stranded DNA. This property of the protein, however, could not account for all of the observed stimulation as it was possible to develop reaction conditions under which strand exchange was still SF1 dependent but the aggregation of double-stranded DNA did not occur.

One of the central intermediates of genetic recombination is the heteroduplex DNA joint [for representative reviews, see Fogel et al. (1981) and Orr-Weaver and Szostak (1985)]. Extensive genetic and biochemical analysis has indicated that a unique class of proteins—the strand exchange proteins—catalyzes the formation of such joints (Radding, 1982; Smith, 1988). The mechanism of action of the strand exchange proteins is best exemplified by the *Escherichia coli* RecA protein (Radding, 1982; Cox & Lehman, 1987; Griffith & Harris, 1988) and T4 bacteriophage UvsX protein (Yonesaki et al., 1985; Formosa & Alberts, 1986; Griffith & Harris,

† This work was supported by an American Cancer Society postdoctoral fellowship to D.N. and by NIH Grant GM29383 to R.K.

* To whom correspondence should be addressed at the Dana-Farber Cancer Institute.

0006-2960/90/0429-7903$02.50/0